INTL JOURNAL OF ELECTRONICS AND TELECOMMUNICATIONS, 2024, VOL. 70, NO. 3, PP. 643–648
Manuscript received May 20, 2024; revised June, 2024. doi: 10.24425/ijet.2024.149591

Origin and properties of own error signals of the discrete wavelet transform algorithms

Łukasz Dróżdż, and Jerzy Roj

***Abstract*—The article presents a method for analyzing the own errors of the discrete wavelet transform algorithms, which are introduced by these algorithms into the output quantities. The presented considerations include determining the origin of the error signals in question and determining their parameters. Both errors resulting from imperfections in the transmittance of the algorithm and those resulting from its implementation in the actual measurement chain were considered.**

***Keywords*—wavelet transform; uncertainty budget; uncertainty estimation; wavelet transform own errors**

I. Introduction

As wavelet transform (WT) algorithms find their applications in many areas [1]–[5], the impact of the discussed algorithms on the uncertainty budget of the measurement chains in which the discussed algorithms are used is extremely important.

In previous works [6]–[8], it was discussed in detail how wavelet transform algorithms transfer error signals contained in the input quantities to the output and it was indicated how to describe the metrological properties of measurement chains containing the algorithms in question in their structure, in order to it was possible to prepare an uncertainty budget and determine the resulting expanded uncertainty value of the output values of the analyzed measurement chains. The considerations presented so far took into account the own errors of the analyzed algorithms only superficially – they did not discuss, among other things, the role of the algorithm's transmittance, and only errors analyzed resulted from its implementation and rounding introduced during calculations was discussed briefly.

This work complements the previous considerations and is devoted to the origins and properties of own error signals of wavelet transform algorithms. The work has been divided into 5 chapters. The first chapter is an introduction to the work and presents its motivation. The second chapter shows the division of own error signals according to their origin. The third chapter describes the properties of the algorithm's own error signals, resulting from the imperfections of the algorithm's transmittance. The fourth chapter discusses the properties of own error signals related to the implementation of the algorithm and the related rounding when performing calculations. Chapter five is a summary of the work.

As the discrete wavelet transform (DWT) is the most frequently used version of the analyzed algorithms [2], all examples presented in the work concern this version of the algorithm. It should be noted, however, that the analysis method discussed in this work is uniform in the case of other variants of the algorithm processing input data belonging to the domain of real numbers.

L. Dróżdż, J. Rój are with Department of Measurement Science, Electronics and Control, Silesian University of Technology, Gliwice, Poland (e-mail: lukasz.drozdz, jerzy.roj@polsl.pl).

II. Genesis of the own error signals

Wavelet transform algorithms can be treated as a set of finite impulse response (FIR) filters [9]. Each output quantity is associated with an appropriate filter, and for the output quantities associated with the same iteration of the decomposition process, the parameters for the corresponding filter are identical [6]. The number of filters therefore depends on the number N_d of iterations of the signal decomposition process and, in general, is equal to $N_d + 1$. The given property does not apply if the transmittance of the algorithm is additionally modified (e.g. an additional measurement window function is introduced, modifying subsequent input values of the algorithm). Therefore, the operation scheme of the discussed algorithm can be presented in the classic case as in the Fig. 1.

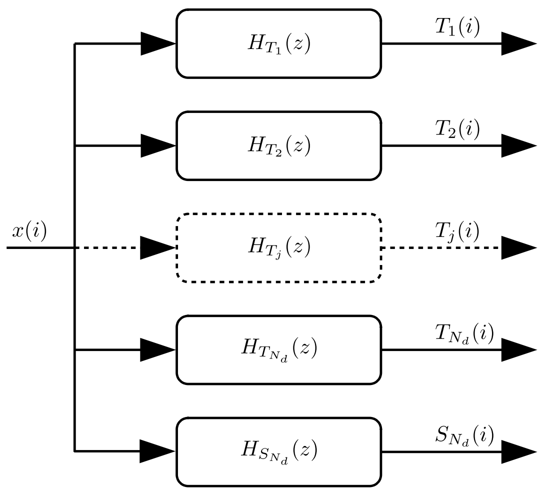

Fig. 1. A block diagram illustrating the operation of the wavelet transform algorithm, where $H_*(z)$ denotes the transmittance associated with the selected output quantity, T_j denotes details and S_j denotes approximations for the given j-th scale number

The model of the wavelet transform algorithm presented in the Fig. 1 simplifies the analysis of the metrological properties of this algorithm, which result from the transmittance associated with its subsequent output quantities. It should be noted, however, that in reality these algorithms usually transform N of input quantities into M of output quantities (where in most cases $N = M$) for each k-th implementation of the analyzed algorithm. The difference between the operation presented in the Fig. 1 and the actual implementation of the algorithm is the fact that for each output quantity of the algorithm, an appropriate filter is used, to which only selected input quantities are fed [2]. As the described property does not affect the transmittance associated with the subsequent output quantities of the actual algorithm, the model presented in Fig. 1 allows for simplifying the analysis without the negative results resulting from this simplification.

In the general case, the transmittance associated with a single i-th output quantity of the algorithm can be described as [6]:

$$H_i(z) = \sum_{j=0}^{N-1} a_{i,j} z^{-j}, \tag{1}$$

where the symbol $a_{i,j}$ denotes the coefficients of the transformation matrix of the algorithm, described in more detail in the works [6], [7]. Based on the equation (1), the value of the j-th output quantity $X(j)$ for the k-th implementation of the algorithm can be described as:

$$X(j) = \sum_{i=0}^{N-1} a_{i,j} x(i), \tag{2}$$

where the symbol $x(i)$ denotes subsequent input quantities of this algorithm.

If the measurement task performed by the measurement chain requires a specific form of transmittance $\dot{H}_j(z)$ for the analyzed output quantity, but the actual form of this transmittance $\tilde{H}_j(z)$, resulting from the properties of the analyzed algorithm, is different (where $\tilde{H}_j(z) \neq \dot{H}_j(z)$), the first source of the algorithm's own error signal can be distinguished. In such a case, it is possible to describe this signal in a deterministic way, which is presented in the next chapter of the work.

Analyzing the Equation (2), it can be noticed that determining the value of the algorithm's output quantity each time requires N multiplication operations and N addition operations. Since the actual implementation of the algorithm usually uses a microcontroller or microprocessor [10]–[14], rounding is associated with these operations, which is the genesis of the second significant error signal [15]. The nature of the signals discussed and their properties are described in the fourth chapter of the work.

The last case requiring discussion is the discrepancy between the numerically and analytically determined values of the coefficients $a_{i,j}$ of the transformation matrix of the algorithm. As shown in the works [2], [6], [16], the origin of the problem is the fact that the values of the discussed coefficients, resulting from the properties of the mother wavelet used and the algorithm parameters, are most often immeasurable. As the discussed discrepancies are very small and are comparable to the value of the numerical error, it is proposed not to analyze these discrepancies as a difference between the ideal and the actual form of the algorithm's transmittance. However, it is proposed to include the contribution of the discussed phenomenon in the analysis of rounding error signals.

III. Errors related with algorithm's transmittance

As indicated in the previous chapter, if the actual form of the algorithm's transmittance differs from that assumed by the designer of the measurement chain, the algorithm will introduce its own errors into the output values. Assuming that the subsequent input quantities of the algorithm are described by the equation:

$$x(i) = \sum_{l=0}^{\infty} E_{x,l} \sin\left(\omega_{x,l} n + \varphi_{x,l}\right), \tag{3}$$

where $T_s = \frac{1}{f_s}$ is the sampling period, appropriate for the sampling frequency f_s, in the case of ideal transmittance $\dot{H}_j(z)$ for the j-th output quantity it can be written:

$$\dot{X}_j(i) = \sum_{l=0}^{\infty} \dot{K}_j\left(\omega_{x,l}\right) E_{x,l} \sin\left(\omega_{x,l} i T_s + \varphi_{x,l} + \dot{\varphi}_j\left(\omega_{x,l}\right)\right), \tag{4}$$

while in the real case:

$$\tilde{X}_j(i) = \sum_{l=0}^{\infty} \tilde{K}_j\left(\omega_{x,l}\right) E_{x,l} \sin\left(\omega_{x,l} i T_s + \varphi_{x,l} + \tilde{\varphi}_j\left(\omega_{x,l}\right)\right). \tag{5}$$

The values of the gain $K_j(\omega)$ and the phase shift $\varphi_j(\omega)$ can be determined based on the transmittance $H_j(z)$ assuming $z = e^{j\omega T_s}$ [17]–[19], then:

$$K_j(\omega) = \left| H_j\left(e^{j\omega T_p}\right) \right| = \sqrt{\left(\Re\left(H_j\left(e^{j\omega T_p}\right)\right)\right)^2 + \left(\Im\left(H_j\left(e^{j\omega T_p}\right)\right)\right)^2}, \tag{6}$$

$$\varphi_j(\omega) = \arctan\left(\frac{\Im\left(H_j\left(e^{j\omega T_p}\right)\right)}{\Re\left(H_j\left(e^{j\omega T_p}\right)\right)}\right). \tag{7}$$

By defining the own error $e_{X_j,h}(i)$, resulting from the imperfection of the algorithm's transmittance, as the difference between the ideal (4) and the actual (5) course of the output quantity $X_j(i)$, it can be written:

$$e_{X_j,h}(i) = \tilde{X}_j(i) - \dot{X}_j(i). \tag{8}$$

Taking into account the content of the Equation (1) and Equation (2), the Equation (8) can also be written in the form:

$$e_{X_j,h}(k) = \sum_{i=0}^{N-1} \left(\tilde{a}_{i,j} x(i+kN) - \dot{a}_{i,j} x(i+kN)\right), \tag{9}$$

where the values of the transformation matrix coefficients $\dot{a}_{i,j}$ in the ideal case correspond to the transmittance $\dot{H}_j(z)$, while the values $\tilde{a}_{i,j}$ correspond to the transmittance $\tilde{H}_j(x)$ in the real case.

Analyzing the content of the Equation (8), we can distinguish subsequent harmonics of the error signal $e_{X_j,h}(i)$, each of which will consist of two components. These harmonics can be described in the form:

$$e_{X_j,h,l}(i) = \tilde{K}_j(\omega_{x,l}) E_{x,l} \sin\left(\omega_{x,l} i T_s + \varphi_{x,l} + \tilde{\varphi}_j(\omega_{x,l})\right) - \dot{K}_j(\omega_{x,l}) E_{x,l} \sin\left(\omega_{x,l} i T_s + \varphi_{x,l} + \dot{\varphi}_j(\omega_{x,l})\right) \quad (10)$$

$$e_{X_j,h}(i) = \sum_{l=0}^{\infty} e_{X_j,h,l}(i), \quad (11)$$

where the symbol l denotes the index of the analyzed harmonic, the pulsation of which is equal to $\omega_{x,l}$. It can be seen that the number of harmonics of the signal $e_{X_j,h}(i)$ depends on the form of the signal $x(i)$. By determining the resultant amplitude $E_{X_j,h,l}$ and the phase shift $\varphi_{X_j,h,l}$ for the l-th harmonic of the signal $e_{X_j,h}(i)$ with pulsation $\omega_{x,l}$ in the form:

$$E_{X_j,l,a} = E_{x,l}\tilde{K}_j(\omega_{x,l}) \cos\left(\varphi_{x,l} + \tilde{\varphi}_j(\omega_{x,l})\right) - E_{x,l}\dot{K}_j(\omega_{x,l}) \cos\left(\varphi_{x,l} + \dot{\varphi}_j(\omega_{x,l})\right), \quad (12)$$

$$E_{X_j,l,b} = E_{x,l}\tilde{K}_j(\omega_{x,l}) \sin\left(\varphi_{x,l} + \tilde{\varphi}_j(\omega_{x,l})\right) - E_{x,l}\dot{K}_j(\omega_{x,l}) \sin\left(\varphi_{x,l} + \dot{\varphi}_j(\omega_{x,l})\right), \quad (13)$$

$$E_{X_j,l} = \sqrt{E^2_{X_j,l,a} + E^2_{X_j,l,b}}, \quad (14)$$

$$\varphi_{X_j,l} = \arctan\left(\frac{E_{X_j,l,a}}{E_{X_j,l,b}}\right), \quad (15)$$

$$e_{X_j,h,l}(i) = E_{X_j,l} \sin\left(\omega_{x,l} + \varphi_{X_j,l}\right). \quad (16)$$

the value of the variance of this harmonic for $\omega_{x,l} > 0$ rad can be determined according to the relationship [18]:

$$\sigma^2_{X_j,h,l} = \frac{1}{2} E^2_{X_j,l}, \quad (17)$$

while the value of the expanded uncertainty related to the analyzed harmonic is equal [20]:

$$U_{X_j,h,l} = c_d \sigma_{X_j,h,l}, \quad (18)$$

where c_d is the coverage factor of the sine function distribution for the assumed confidence level $\gamma = 1 - \alpha$ [20].

In the case where $\omega_{x,l} = 0$ rad the Equation (10) simplifies to the following form:

$$e_{X_j,h,0}(i) = \tilde{K}_j(0) E_{x,l} \sin\left(\varphi_{x,l} + \tilde{\varphi}_j(0)\right) - \dot{K}_j(0) E_{x,l} \sin\left(\varphi_{x,l} + \dot{\varphi}_j(0)\right). \quad (19)$$

For this case, the variance $\sigma^2_{x,0}$ of the constant signal component $x(i)$ should be determined, the realization values of which may change for subsequent measurement series, and then according to the equation:

$$\sigma^2_{X_j,h,0} = \left(\tilde{K}_j(0) - \dot{K}_j(0)\right)^2 \sigma^2_{x,0}. \quad (20)$$

As the transmittance of the analyzed object is linear and time invariant [19], the expanded uncertainty value in the discussed case can be determined according to the equation:

$$U_{X_j,h,0} = \sigma_{X_j,h,0} c_{x,0}, \quad (21)$$

where $c_{x,0}$ is the coverage factor for the probability density distribution of the realization of the constant component of the signal $x(i)$.

As the successive harmonics of the error signal $e_{X_j,h}(i)$ are not correlated [18], [19], the variance of this signal is described by the relationship:

$$\sigma^2_{X_j,h} = \sum_{l=0}^{\infty} \sigma^2_{X_j,h,l}. \quad (22)$$

The resulting expanded uncertainty for the analyzed error signal can be determined using the Monte Carlo method [21], [22], the method using fuzzy sets [23], the reduction interval arithmetic method [6] or any other method.

IV. ERRORS RELATED WITH ALGORITHM'S IMPLEMENTATION

No microprocessor or microcontroller can achieve infinite precision in computing floating-point numbers. In practice, this means that every arithmetic operation that the device performs on the numbers in question involves introducing an error into the result. This error can be interpreted as the difference between the value obtained by the device and the value obtained assuming infinite precision of numbers [15]. As indicated in the first chapter of the work, the output values of the wavelet transform algorithm are determined according to the Equation (2). Theoretically, determining the value of the implementation of a single output quantity of the analyzed algorithm involves N multiplication operations and N addition operations. In practice, however, this value does not correspond to the real number of arithmetic operations, because some of the coefficients of the transformation matrix for the selected output quantity have a value equal to 0 , which is explained later in the chapter.

Analyzing the information compiled in the works [2], [3], [6], [7], [9], [16], it can be noticed that each mother wavelet for given parameters is characterized by a certain number of non-zero scaling factors, the numbers and values of which depend on the values of the transformation matrix coefficients algorithm. While the number of non-zero scaling factors is constant for the given mother wavelet parameters, the number and values of non-zero transformation matrix coefficients are also influenced by the number of input quantities of the algorithm and the number of iterations of the signal decomposition process.

According to the content presented in the first paragraph of this chapter, one important problem should be noted. Since each digital device will introduce an error into the calculations due to the limited precision of number recording, the use of such a device in an experiment aimed at determining the parameters of the signal related to the rounding in question is impossible. However, it is proposed to perform an appropriate experiment in the case when the precision of writing numbers

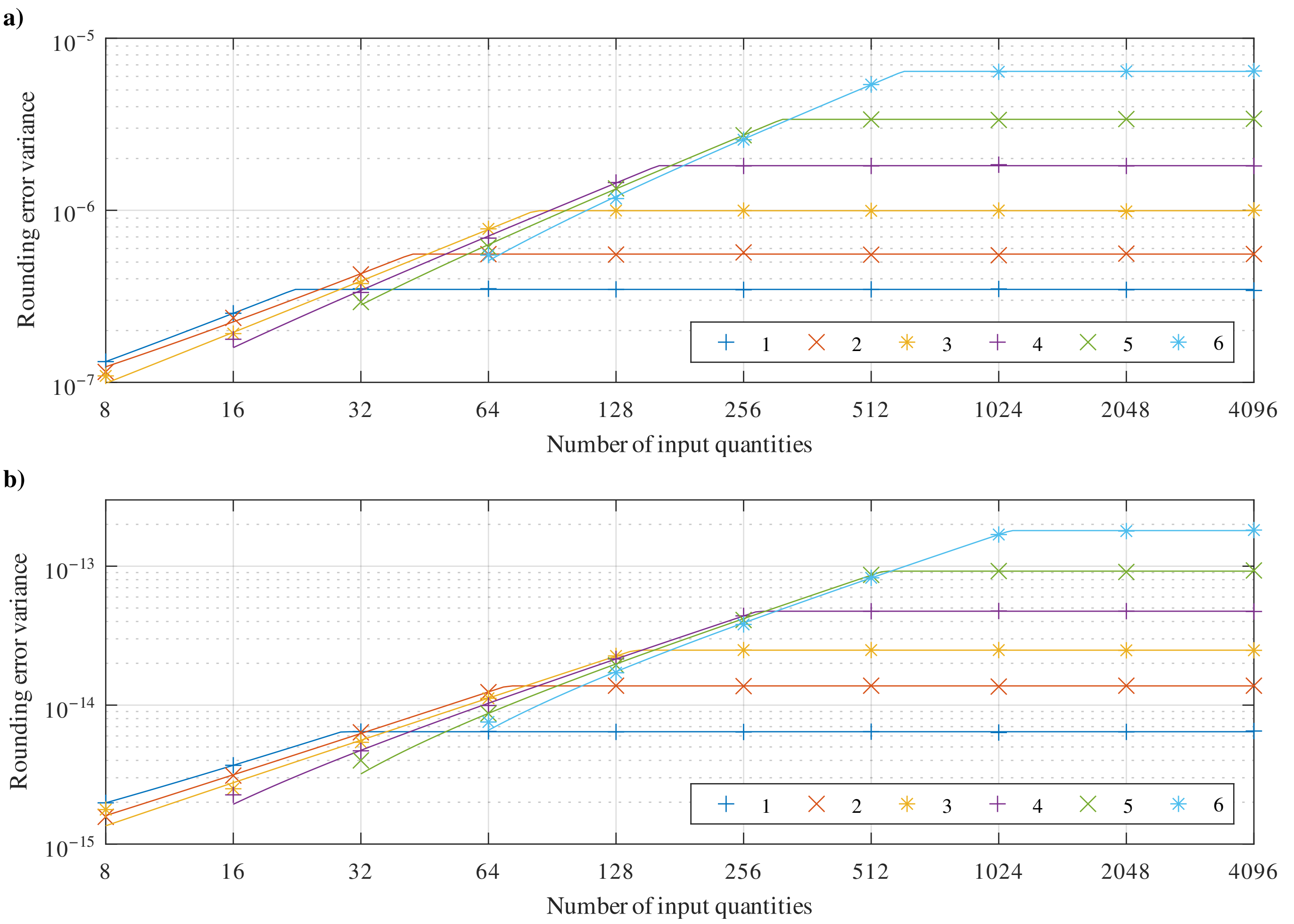

Fig. 2. Dependence of the value of the rounding error signal variance on the number of iterations of the signal decomposition process and the number of input quantities for the "coif5" wavelet when using floating-point numbers with a word length of **a)** 16 bits and **b)** 32 bits for the last scale of signal details

used to determine reference values (considered as ideal) will be much higher than in the case of the real algorithm. For the described experimental conditions, it can be assumed that the errors introduced in the ideal part will be many orders of magnitude smaller than in the real part, and therefore the experiment will allow to estimate the parameters of the analyzed error signal [15], [20].

Assuming that the input quantities $x(i)$ of the algorithm are not burdened with any error signal, and the transfer function of the algorithm is ideal (the difference between the ideal and real values of the transformation matrix coefficients is very small, i.e. many orders of magnitude smaller than those described in previous chapter), the error signal $e_{X_j,z}(i)$ related with the j-th output quantity of the algorithm can be defined as:

$$e_{X_j,z}\left(i\right) = \tilde{X}_j\left(i\right) - \dot{X}_j\left(i\right), \tag{23}$$

where $\tilde{X}_j(i)$ denotes the output value of the tested algorithm, while $\dot{X}_j(i)$ denotes the output value of the reference algorithm (for which much greater precision is used writing numbers). Further in the work, it was assumed that the ideal (reference) algorithm will use real numbers with a word length of 128 bits. All described research was performed using implementations of algorithms in "C", which were translated into machine code using the "GNU GCC" [24] compiler.

The first analyzed phenomenon is the influence of the number of input quantities of the algorithm on the value of the error signal variance, described by the Equation (23). The second analyzed phenomenon is the influence of the number of iterations of the signal decomposition process on the discussed parameters. In order to determine the variance and shape of the probability density function of obtaining the selected realization of the error signal $\tilde{X}_j(i)$, a vector of input quantities of the algorithm was generated, the realization values of which were random numbers in the range $\hat{x}(i) \in [-1; 1]$ with the same probability of obtaining each value. For a given vector of input values, the vector of output values of the ideal and real algorithm was determined, and for the real algorithm floating-point numbers with a word length of 16 or 32 bits were used (depending on the experiment variant). Based on the Equation (23), the implementations of the analyzed error signal was determined for the current iteration of the experiment using 100,000 samples for each variant.

The above experiment was performed for the wavelet "coif5" (the 5-th order "Coiflet" wavelet [25]). The wavelet in question has 30 non-zero scaling factors. Depending on the experiment variant, the number of input quantities for the algorithm was $\hat{N} \in \{8;16;32;64;128;256;512;1024;2048;4096\}$, while the number of iterations of the input signal decomposition process was $\hat{N}_d \in [1;6]$. The value of the error signal variance $\sigma^2_{X_j,z}$ depending on the experiment variant is shown on Fig. 2. Based on the experiment, it can be seen that for the selected number of iterations of the signal decomposition process, the value of the variance of the error signal $e_{X_j,z}(i)$ increases with the increase in the number of input quantities of the algorithm. However, it can be noted that this increase only occurs when the number of input quantities does not exceed the number of non-zero coefficients of the algorithm's transformation matrix. As the number of non-zero coefficients of the algorithm's transformation matrix increases for the final output scale as the number of iterations of the signal decomposition process increases, the number of arithmetic operations that introduce rounding errors also increases. Additionally, it can be noted that the variance of the own error signal in the case of the implementation using 32-bit floating-point numbers is much smaller than in the case of the algorithm using 16-bit numbers.

Another problem requiring discussion is the influence of the range of implementation values of the algorithm's input quantities on the value of the rounding error signal variance. To verify the phenomenon in question, an experiment was performed in which the vector of input quantities were random numbers from the range $\hat{x}(i) \in [-b;b]$ with the same probability of obtaining each value. The value of b changed for each variant of the experiment, and for the selected variant the parameters of the signal $e_{X_j,z}(i)$ were determined on the basis of 100,000 values of the signal in question implementations. Fig. 3 show selected experimental results for the output values of the algorithm using the "db2" wavelet (the 2-nd order "Daubechies" wavelet [16]) for 2 iterations of the signal decomposition process and 128 input quantities. Based on the presented results, one can notice an increase in the variance of the analyzed error signal with an increase in the range of possible implementation values of the algorithm's input quantities, and this trend can be approximated by a second-order polynomial.

The last experiment was aimed at verifying the algorithm model presented earlier in Fig. 1. The presented model assumes that the transmittance of all output quantities related to the same scale parameter is identical, and the only difference when determining the value of the output quantity is therefore the set of data fed to the input of this transmittance. Therefore, the variance of the rounding error signal should be identical for quantities associated with the same transmittance. In order to verify this thesis, an experiment was carried out in which a vector of input quantities was fed to the algorithm, the subsequent implementation values of which were in the interval $\hat{x}(i) \in [-b;b]$ with the same probability of obtaining each value, with the b values depending on the experiment variant. The algorithm processed $N = 8$ input quantities using the "db2" wavelet for 2 iterations of the signal decomposition process. The experimental results are summarized in Table I. Based on the results obtained, the thesis in question can be considered true. The discrepancies obtained result from the features of the Monte Carlo method [22].

TABLE I
ROUNDING ERROR SIGNAL VARIANCE VALUES FOR THE "DB2" WAVELET FOR NUMBERS WITH A LENGTH OF **A)** 16 BITS AND **B)** 32 BITS, DEPENDING ON THE RANGE OF POSSIBLE VALUES OF THE IMPLEMENTATION OF THE INPUT QUANTITIES

Case	X_j	Input value range		
		$\hat{x} \in [-1;1]$	$\hat{x} \in [-2;2]$	$\hat{x} \in [-3;3]$
a)	$S_{2,0}$	1.03×10^{-7}	4.12×10^{-7}	9.74×10^{-7}
	$S_{2,1}$	1.11×10^{-7}	4.43×10^{-7}	1.01×10^{-6}
	$T_{2,0}$	1.31×10^{-7}	5.24×10^{-7}	1.21×10^{-6}
	$T_{2,1}$	1.07×10^{-7}	4.29×10^{-7}	9.73×10^{-7}
	$T_{1,0}$	7.09×10^{-8}	2.85×10^{-7}	6.99×10^{-7}
	$T_{1,1}$	5.83×10^{-8}	2.33×10^{-7}	5.87×10^{-7}
	$T_{1,2}$	5.84×10^{-8}	2.34×10^{-7}	5.85×10^{-7}
	$T_{1,3}$	5.53×10^{-8}	2.21×10^{-7}	5.41×10^{-7}
b)	$S_{2,0}$	1.40×10^{-15}	5.57×10^{-15}	1.30×10^{-14}
	$S_{2,1}$	1.40×10^{-15}	5.61×10^{-15}	1.29×10^{-14}
	$T_{2,0}$	1.71×10^{-15}	6.83×10^{-15}	1.58×10^{-14}
	$T_{2,1}$	1.39×10^{-15}	5.56×10^{-15}	1.29×10^{-14}
	$T_{1,0}$	8.28×10^{-16}	3.54×10^{-15}	8.38×10^{-15}
	$T_{1,1}$	6.82×10^{-16}	2.72×10^{-15}	6.67×10^{-15}
	$T_{1,2}$	6.82×10^{-16}	2.72×10^{-15}	6.66×10^{-15}
	$T_{1,3}$	6.68×10^{-16}	2.67×10^{-15}	6.48×10^{-15}

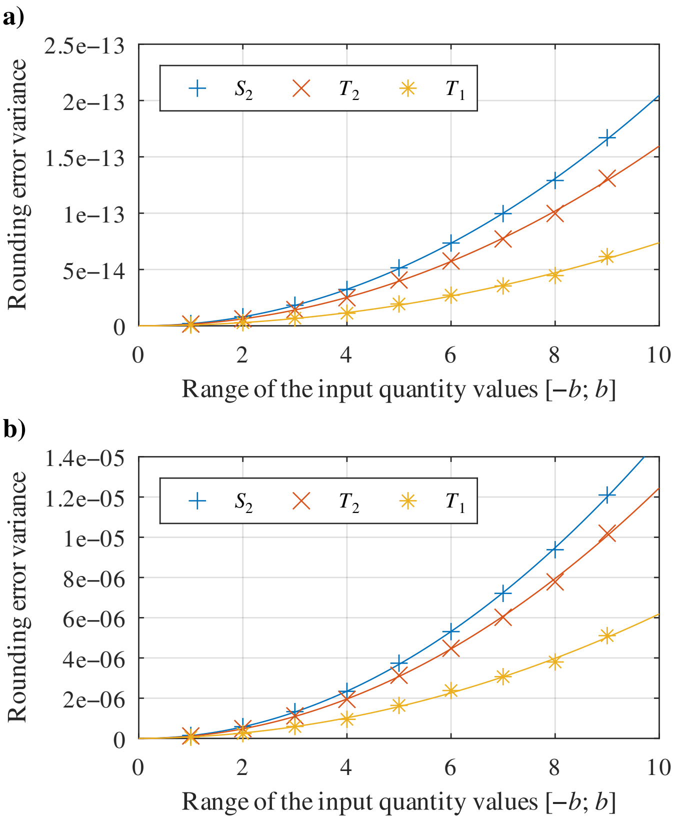

Fig. 3. Dependence of the rounding error signal variance value on the range of the input quantities implementation values for the "db2" wavelet using floating-point numbers with a word length of **a)** 16 bits and **b)** 32 bits

The last issue is to determine the value of the coverage factor for the analyzed own error signals. Based on the experiments performed, it can be estimated that the value of the discussed coefficient is approximately $c_z \approx 2.15$ for confidence level $1-\alpha = 95\%$, while the exact value depends on the parameters of the wavelet transform algorithm used and its implementation. The probability density distribution of the signal in question is therefore close to the normal distribution.

V. Conclusions

The article describes both error signals resulting from imperfections in the transmittance of the wavelet transform algorithm, as well as those resulting from the actual implementation conditions of this algorithm. The origin of the first group of error signals is the fact that the actual transmittance of the algorithm does not always coincide with the transmittance required by the measurement task. The role of the measurement chain designer is to determine the ideal transmittance of the algorithm for the task being performed and then, in accordance with the presented methodology, to determine the uncertainty budget related to the discrepancy in question. In the case of the second group of error signals, their origin results from the inability to achieve infinite precision in writing floating-point numbers. When determining the implementation value of the algorithm's output quantities, the calculation results are rounded, which is the origin of the error signal in question.

Analyzing the properties of the own error signal related to rounding, several most important properties of this signal can be noticed. The first property is the dependence of the variance of this signal on the length of the word used to write floating-point numbers. As the length of the word increases, the accuracy of writing numbers increases, and therefore the rounding discussed earlier is characterized by a smaller absolute value and a lower precision compared to previous one. However, it should be noted that as the word length increases, the amount of required memory increases and the computation time increases [11], [15], [24], [26]. Therefore, the precision of number recording should be selected so that the variance of the rounding error is small in relation to other error signals [20]. The second property results from the influence of the range of input values on the variance of the analyzed error signal. For a larger range, the value in question increases with the square of the range increase. The last important issue is the overall impact of the number of non-zero values of the algorithm's transformation matrix coefficients on the value of the rounding error signal variance. The discussed relationship causes an increase in the variance of the rounding own error signal with an increase in the number of input values of the algorithm and the number of iterations of the signal decomposition process. The growth in question can be approximately considered linear.

As the parameters of the own error signals of the wavelet transform algorithm depend largely on the parameters of the processed measurement signal, all experiments aimed at determining the parameters of these signals should take place in conditions similar to those in which the analyzed algorithm operates.

References

[1] K. A. Ahmad, *Wavelet Packets and Their Statistical Applications*. Springer Singapore, 2018.

[2] P. S. Addison, *The illustrated wavelet transform handbook: introductory theory and applications in science, engineering, medicine and finance*, 2nd ed. CRC Press, 2017.

[3] C. M. Akujuobi, *Wavelets and Wavelet Transform Systems and Their Applications*. Springer, 2022.

[4] A. Z. Averbuch, P. Neittaanmäki, and V. A. Zheludev, *Spline and Spline Wavelet Methods with Applications to Signal and Image Processing*. Springer, 2019, vol. 3.

[5] A. Singh, A. Rawat, and N. Raghuthaman, *Mexican Hat Wavelet Transform and Its Applications*. Springer, 2022, pp. 299–317.

[6] L. Dróżdż, M. Kampik, and J. Roj, "Estimation of the resultant expanded uncertainty of the output quantities of the measurement chain using the discrete wavelet transform algorithm," *Applied Sciences*, vol. 14, no. 9, 2024. [Online]. Available: http://doi.org/10.3390/app14093691

[7] L. Dróżdż and J. Roj, "Propagation of random errors by the discrete wavelet transform algorithm," *Electronics*, vol. 10, no. 7, 2021. [Online]. Available: http://doi.org/10.3390/electronics10070764

[8] L. Dróżdż, M. Kampik, and J. Roj, "Error model of a measurement chain containing the discrete wavelet transform algorithm," *Applied Sciences*, vol. 14, no. 8, 2024. [Online]. Available: http://doi.org/10.3390/app14083461

[9] S. Mallat, *A wavelet tour of signal processing*, 3rd ed. Academic Press, 2008.

[10] D. S. Reay, *Digital Signal Processing Using the ARM Cortex M4*. John Wiley & Sons, 2015.

[11] *CMSIS-DSP – Embedded compute library for Cortex-M and Cortex-A*, ARM Limited, 2023.

[12] Z. Průša, P. L. Søndergaard, and P. Rajmic, "Discrete wavelet transforms in the large time-frequency analysis toolbox for matlab/gnu octave," *ACM Transactions on Mathematical Software (TOMS)*, vol. 42, no. 4, pp. 1–23, 2016. [Online]. Available: http://doi.org/10.1145/2839298

[13] M. Misiti, Y. Misiti, G. Oppenheim, and J. M. Poggi, *Wavelet toolbox*, The MathWorks Inc., 2018.

[14] G. Lee, R. Gommers, F. Waselewski, K. Wohlfahrt, and A. O'Leary, "Pywavelets: A python package for wavelet analysis," *Journal of Open Source Software*, vol. 4, no. 36, p. 1237, 2019. [Online]. Available: http://doi.org/10.21105/joss.01237

[15] F. Benz, F. Hildebrandt, and S. Hack, "A dynamic program analysis to find floating-point accuracy problems," *ACM SIGPLAN Notices*, vol. 47, no. 6, pp. 453–462, 2012. [Online]. Available: http://doi.org/10.1145/2345156.2254118

[16] C. Vonesch, T. Blu, and M. Unser, "Generalized daubechies wavelet families," *IEEE Transactions on Signal Processing*, vol. 55, no. 9, pp. 4415–4429, 2007. [Online]. Available: http://doi.org/10.1109/TSP.2007.896255

[17] A. V. Oppenheim and R. W. Schafer, *Discrete-time signal processing*, 3rd ed. Pearson, 2009.

[18] A. V. Oppenheim, A. S. Willsky, and S. H. Nawab, *Signals & Systems*, 2nd ed. Pearson, 2013.

[19] J. G. Proakis and D. G. Manolakis, *Digital Signal Processing: Principles, Algorithms and Applications*, 5th ed. Pearson, 2021.

[20] Joint Committee for Guides in Metrology, *Evaluation of measurement data – Guide to the Expression of Uncertainty in Measurement*, JCGM, 2008. [Online]. Available: https://www.bipm.org/documents/20126/2071204/JCGM_100_2008_E.pdf

[21] H. Janssen, "Monte-carlo based uncertainty analysis: Sampling efficiency and sampling convergence," *Reliability Engineering & System Safety*, vol. 109, pp. 123–132, 2013. [Online]. Available: http://doi.org/10.1016/j.ress.2012.08.003

[22] Joint Committee for Guides in Metrology, *Evaluation of measurement data – Propagation of distributions using a Monte Carlo method*, JCGM, 2008. [Online]. Available: https://www.bipm.org/documents/20126/2071204/JCGM_101_2008_E.pdf

[23] M. K. Urbanski and J. Wąsowski, "Fuzzy approach to the theory of measurement inexactness," *Measurement*, vol. 34, no. 1, pp. 67–74, 2003. [Online]. Available: http://doi.org/10.1016/S0263-2241(03)00021-6

[24] R. M. Stallman *et al.*, *Using the GNU Compiler Collection*, Free Software Foundation, 2023.

[25] D. Wei, *Coiflet-type wavelets: theory, design, and applications*, The University of Texas at Austin, 1998.

[26] *Cortex-M4 – Technical Reference Manual*, ARM Limited, 2010.